Journal of Ceramic Processing Research. Vol. 18, No. 1, pp. 73~78 (2017)

J O U R N A L O F
Ceramic Processing Research

Ferroelectric characterization of $SrBi_2Ta_2O_9$ obtained by microwave processing

Ricson R. Souza[a,*], Daniel Thomazini[b], Maria V. Gelfuso[b], Harvey Amorín[c], Altair S. Pereira[d] and Vânia C. Sousa[a]

[a]*Engineering Department, Federal University of Rio Grande do Sul (UFRGS), Porto Alegre, Rio Grande do Sul, Brazil*
[b]*Mechanical Engineering Institute, Federal University of Itajubá (UNIFEI), Itajubá, Minas Gerais, Brazil*
[c]*Instituto de Ciencia de Materiales de Madrid (ICMM), CSIC, Madrid, Spain*
[d]*Physic Institute, Federal University of Rio Grande do Sul (UFRGS), Porto Alegre, Rio Grande do Sul, Brazil*

Microwave processing is an attractive approach for the production of materials with improved properties, using fast heating curves. In this work, $SrBi_2Ta_2O_9$ samples were obtained by the mixture of oxides (Bi_2O_3, Ta_2O_5 and $SrCO_3$). The microstructural evolution during microwave sintering was investigated by scanning electron microscopy in association with energy dispersion spectroscopy and with the support of an X-ray diffraction analyzer. Frequency response analysis was used to obtain the electric curves and a synthesizer/function generator, in combination with a high voltage amplifier, to obtain the ferroelectric hysteresis measurements. Results show that microwave process proved to be a good alternative to the conventional process to obtain suitable ferroelectric properties. Furthermore, in strontium bismuth tantalate samples sintered at 1200 °C by microwave processing, a berlincourt d_{33} lineal piezoelectric coefficient of 5 pC/N, a remnant polarization P_r of 4 mC/cm^{-2} and a coercive field E_c of 2.6 kV/mm were achieved.

Key words: Microwave, Sintering, Ferroelectric, Oxides, Strontium bismuth tantalate.

Introduction

Ferroelectric materials show a wide range of properties, including spontaneous polarization, piezoelectricity, pyroelectricity, non-linear optical properties and dielectric properties. These characteristics are essential for application in several electronic devices such as sensors, microactuators, infrared detectors, and non-volatile memories [1].

Lead zirconate titanates (PZTs) and their derivatives, with donor or acceptor dopants, are dominant in piezoceramic ultrasonic applications, such as non-destructive tests, medical diagnoses, underwater signalling, etc [2]. However, in recent years, environmental and health issues have been major drivers for the development of high-performance lead-free piezoelectric ceramics [3-6]. Strontium bismuth tantalate (SBT), barium zirconate titanate (BZT), $BaTiO_3$, barium zirconate, ZnO, among others, appear as possible alternatives to PZT.

Strontium bismuth tantalate (SBT), $SrBi_2Ta_2O_9$, is a ferroelectric material that has attracted considerable interest as its polarization can be modified at low voltages and there is no polarization-switching fatigue. Bismuth layer-structured ferroelectrics (BLSFs), which include SBT, belong to the Aurivillius family of mixed bismuth layered perovskites, and have the general formula $(Bi_2O_2)^{2+}$ $(A_{m-1}B_mO_{3m+1})^{2-}$ where m denotes the number of corner-sharing octahedral-forming perovskite-like slabs. In particular, the molecular formula for SBT is $(Bi_2O_2)^{2+}(SrTa_2O_7)^{2-}$ where Sr and Ta present coordination numbers 12 and 6, respectively. The electrical properties of the SBT system are widely studied in bulk materials [7-10] and thin films [11-13]. One main consideration in the sintering of SBT using conventional processing is that the addition of excess bismuth oxide can compensate stoichiometric losses of the compound and contribute to improving the electrical properties [14-20].

In the microwave heating process, the heat is generated from the interior part of the material instead of the surface part, and hence there is an inverse heating profile. Microwave process has many advantages over conventional heating methods, for example, they include high heating rate, followed by sintering in a short period of time, enhanced densification rate, decreased sintering active energy and smaller grain size than those obtained by conventional sintering [21-24].

The purpose of this article is to study the influence of the microstructure in the ferroelectric properties of $SrBi_2Ta_2O_9$ samples sintered by microwave processing.

Materials and Methods

Bi_2O_3 (P.A.,Vetec) and Ta_2O_5 (99%, Vetec) powders were mixed in an equal molar ratio (1 : 1), and ball-milled for 6hrs, using a polyethylene jar, containing distilled water and zirconia balls. The solid volume / water volume ratio, inside the polyethylene jar, was 1 : 1. After mixing, the entire jar's content was removed,

*Corresponding author:
Tel : +55 51 3308 9485
E-mail: ricson.souza@ufrgs.br

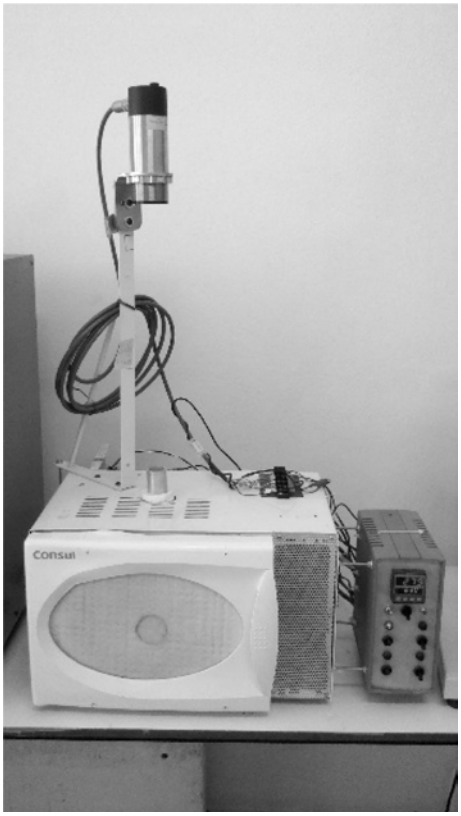

Fig. 1. Microwave oven adapted for sintering of ceramics samples.

dried at 110 ºC for 24 hrs in air to evaporate water, and passed through a 325-mesh sieve. The dried mixture was calcined in an electrical furnace in air at 900 ºC for 2 hrs, using a heating rate of 10 ºC/min, to obtain $BiTaO_4$. The $BiTaO_4$ powder was subsequently mixed with $SrCO_3$ in the stoichiometric ratio corresponding to $SrBi_2Ta_2O_9$. This mixture was then submitted to the same previous ball-milling and drying processes and compacted at 200 MPa into pellets of 10 mm in diameter and about 3.4 mm thick. After this compaction, the samples were heated at a rate of 1000°C/min and sintered at 1100 ºC and 1200 ºC, for 1 hr. The microwave sintering was performed using a microwave oven adapted to burn with heating rates of 1000 ºC/min and to reach a maximum temperature of 1650 ºC (Fig. 1).

After microwave processing, an Arquimedes technique was used to determine the relative density of the sintered samples. The surface of the samples was polished with diamond paste (6 μ, 1 μ and 1/4 μ). Then, the phase identification of the processed samples was done by X-ray diffraction (XRD) analysis, using a Siemens D500 diffractometer, equipped with a Cu X-ray tube and a graphite monochromator. The microstructural evaluation was performed by scanning electron microscopy, model JSM 5800, associated with energy dispersive X-ray spectroscopy (SEM/EDS), with an operation voltage of 20 kV. Before starting the electrical characterizations, silver paste was deposited on both parallel faces of the samples and submitted to thermal treatment at 600 ºC per 15 min, to be used as contact electrodes. Then, samples were placed in an oven (Inti-Maitec, model FT -1.000/3) for electrothermic testing to 1000 °C, coupled to equipment for frequency response analysis (FRA), an Autolab PGSTAT302N with FRA32M module. The electric measurements of the ceramics were carried out in a frequency range between 1 Hz and 1 MHz, in a temperature range of 25 ºC to 525 ºC. The FRA equipment was employed. For ferroelectric hysteresis measurements, high voltage sine waves with 0.1 Hz (up to 10 kV/mm) and 0.01 Hz (up to 12 kV/mm) were applied by the combination of a synthesizer/function generator (HP 3325B) and a high voltage amplifier (Trek model 10/ 40A), and charge was measured with homebuilt charge to voltage converter and software for loop acquisition and analysis.

Results

After the reaction between Bi_2O_3 and Ta_2O_5, a $BiTaO_4$ phase was obtained, as the XRD pattern shows in Fig. 2. The formation of this intermediate compound

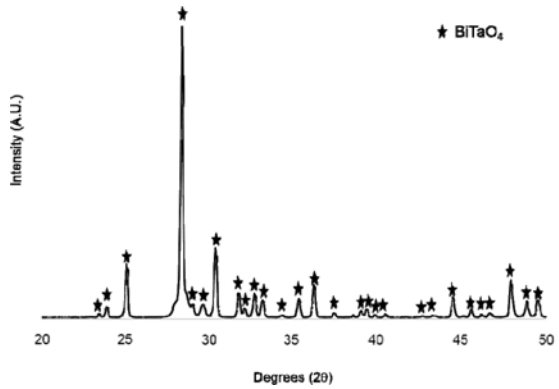

Fig. 2. X-ray diffraction pattern obtained by reaction between Bi_2O_3 and Ta_2O_5 calcined at 900 ºC for 2 hrs.

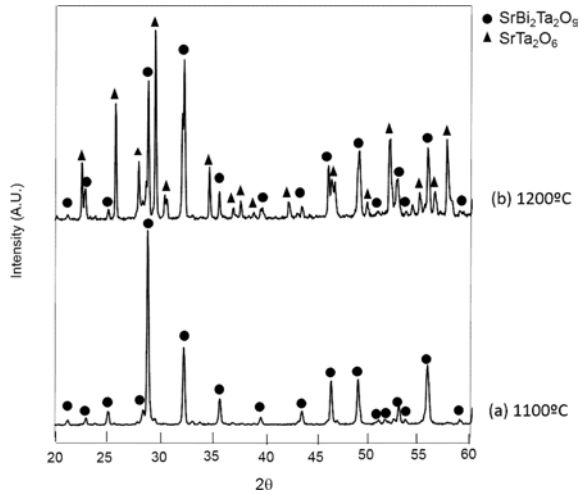

Fig. 3. X-ray diffraction patterns of samples processed by microwave sintering, varying temperature.

Table 1. Physical properties of samples sintered by microwave processing.

	Apparent porosity (%)	Water absorption (%)	Apparent density (g/cm^3)	Theoretical density (g/cm^3)	Relative density (%)
1100 ºC	28.50 ± 3.81	4.90 ± 0.66	5.80 ± 0.01	8.78	66 ± 0.06
1200 ºC	2.40 ± 1.39	0.30 ± 0.18	8.00 ± 0.17	8.78	91 ± 1.97

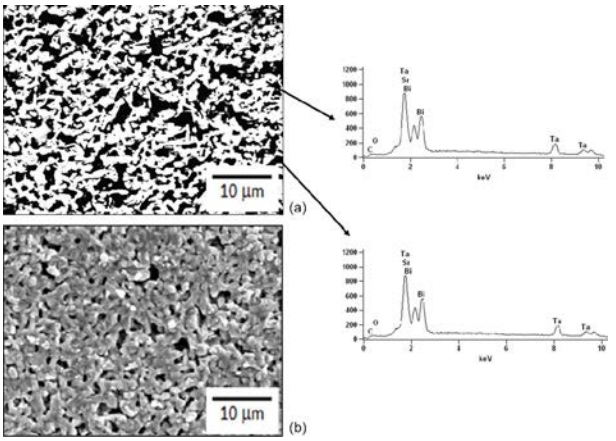

Fig. 4. (a) SEM micrograph (backscattered electrons imaging) of the sample sintered at 1100ºC including energy dispersive X-ray spectra taken from the indicated regions. (b) Secondary electrons imaging of the same area as in (a). Characteristic peak at 2 keV is attributed to gold sputtering on the surface.

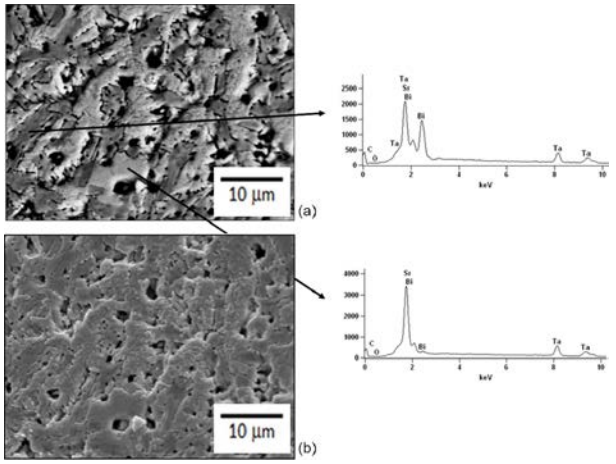

Fig. 5. (a) SEM micrograph (backscattered electrons imaging) of the sample sintered at 1200ºC including energy dispersive X-ray spectra taken from the indicated regions. (b) Secondary electrons imaging of the same area as in (a). Characteristic peak at 2 keV is attributed to gold sputtering on the surface.

is an essential step in the formation of SBT from the subsequent reaction with $SrCO_3$.

The XRD patterns in Fig. 3 of samples processed by microwave sintering showed very different patterns. From the analysis of the diffraction patterns it was possible to identify a multiphasic system after sintering, in temperatures above 1100 ºC, with the presence of peaks related to the $SrBi_2Ta_2O_9$ and $SrTa_2O_6$ phases. Already at sintering temperatures below 1100 ºC a monophasic system prevailed, with the presence of a $SrBi_2Ta_2O_9$ phase.

After sintering, the densities of the samples sintered by microwave sintering were measured by the Archimedes method. Measurements carried out in samples sintered at 1100 ºC and 1200 ºC revealed a relative density of 66 ± 0.06% and 91 ± 1.97%, respectively. Table 1 shows that, despite the formation of a monophasic system, sintering at 1100 ºC for 1 hour by the microwave process proved insufficient to ensure a high densification. In contrast, sintering at 1200 ºC, although forming a multiphasic system, conferred an increase in densification and there is clearly a decrease in porosity and water absorption.

This indication is in accordance with studies on SBT samples, which show a relative density of around 90% between 1100 ºC and 1300 ºC, even with a multiphasic system. It is important to consider that the addition of bismuth excess could contribute to the increase in densification [16-17, 25].

The SEM/EDS analysis of a sample sintered at 1100 ºC (Fig. 4) indicated microstructural homogeneity and high porosity. The high similarity between the characteristic X-ray spectra taken from different regions of the sample, and the homogeneous Bi distribution shown by the corresponding X-ray map (Fig. 4(b)), are in agreement with the XRD results (Fig. 4), which indicate the presence of a single-phase, $SrBi_2Ta_2O_9$, in this sample. No evidence for bismuth volatilization was found in this processing condition.

In relation to the sample sintered at 1200 ºC (Fig. 5) it was possible to observe a microstructural heterogeneity, indicating stoichiometric loss and the presence of distinct phases in the microstructure, prevailing regions poor in bismuth, which can be attributed to the $SrTa_2O_6$ phase (Fig. 3). The bismuth X-ray map reveals clearly the stoichiometric decomposition mentioned (Fig. 5(b)). Samples sintered at higher temperatures (1200 ºC) by microwave sintering technique exhibit a porous morphology and slightly packaged [26-31]. This may be related to the fact that the sintering mechanism to be fundamentally different from conventional sintering [32]. Analyzing the surface of these heterogeneous samples, it has revealed the presence of strontium tantalate layer with a morphological appearance of grains of the plate type. It is known that the formation of the plate type grain is a typical feature of BLSFs because they exhibit a highly anisotropic crystal structure [26-31]. By microstructural analysis, the samples sintered at 1100 ºC by microwave sintering proved more homogeneous, with a predominance of the SBT phase.

Fig. 6 revealed the dielectric loss as a function of

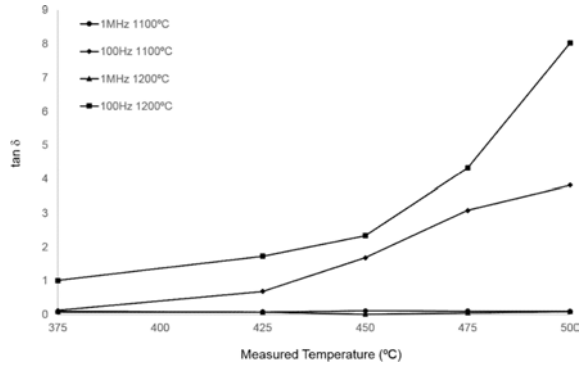

Fig. 6. Dielectric loss of $SrBi_2Ta_2O_9$ (at 1 MHz and at 100 Hz) samples as a function of temperature.

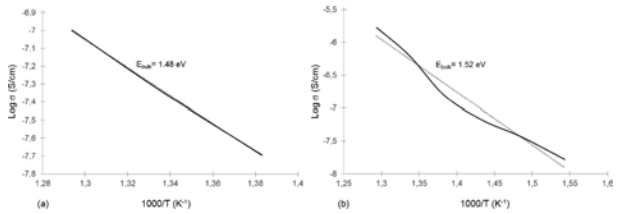

Fig. 7. Temperature-dependence of bulk total conductivity of samples sintered by microwave processing at 1100 ºC (a) and at 1200 ºC (b).

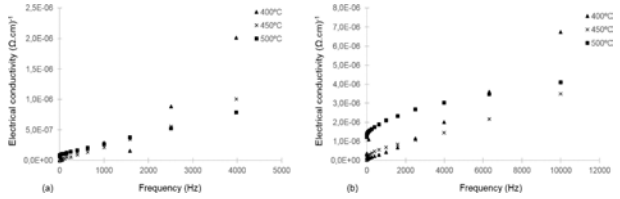

Fig. 8. Frequency dependence of electrical conductivity at different measured temperatures, of samples sintered by microwave processing at 1100 ºC (a) and at 1200 ºC (b).

measured temperature. The sharp increase of dielectric loss in samples sintered at 1200 ºC is attributed to the increased mobility of space charges in the $SrBi_2Ta_2O_9$ sample [32]. Bismuth volatilization in these samples contribute to a higher dielectric loss.

Fig. 7 represents the temperature-dependence of conductivity of $SrBi_2Ta_2O_9$, with the bulk total contribution obtained from the complex impedance planes of samples. The analysis temperatures to obtain curves were close to the regions of the ferroelectric transition, in order to verify the behavior of space charges in the conductivity of the samples. The bulk total activation energy value (grain + grain boundary) was around 1.50 eV for both samples sintered by microwave sintering, which is a typical value for oxygen vacancies ($V_{\ddot{o}}$) in perovskites that, practically, dominate total conductivity of $SrBi_2Ta_2O_9$ [33]. This is because values between 1.0 eV and 1.5 eV are very close to the data found for $SrBi_2Ta_2O_9$ in the literature [7, 33-35] and represent the energy cost of conductivity [33].

It was also observed that the electric conductivity

Table 2. Bulk electric conductivity (s_b) of $SrBi_2Ta_2O_9$ ceramics.

Measured Temperature	Sintering	$\sigma_b \times 10^{-7}$ $(\Omega.cm)^{-1}$
450 ºC	This work at 1100ºC	0.20
450 ºC	This work at 1200 ºC	1.57
425 ºC	Conventional [8] at 1150 ºC	27.74
430 ºC	Conventional [9] at 1230 ºC	2.95

increases with temperature and is also dependent on the frequency of the test (Fig. 8); that is, the higher the frequency, the higher conductivity of the material. With the increase of temperature the electrical conductivity increases because it is a thermally activated magnitude. In addition, it is possible to note a change in the slope of the curves around 1 KHz (at 1100 ºC) and 2 KHz (at 1200 ºC). This change occurs at higher frequency, with increasing temperature.

Additional information about the electric conductivity of $SrBi_2Ta_2O_9$ ceramics can be seen in Table 2, correlating data extracted from the literature. Thus, results indicate lower conductivity values than samples sintered by conventional sintering. It appears that the microwave processing partially decreases the bismuth mass transport mechanism, providing suitable electric characteristics.

It is also known that porosity is a type of defect and that electronic defects, in general, can modify the ferroelectric properties of perovskite compounds [33]. Studies suggest that the presence of pores in ferroelectric ceramics can be regarded as a reservoir of space charges, creating a large area of a free internal surface, which can be favorable for electrical conduction [36-39]. It is also known that variations in sintering temperatures, material-processing techniques, compositions, etc., may affect the densification and microstructure of the samples, affecting the ferroelectric properties of materials [26-31,40-41].

For ferroelectric hysteresis measurements, $SrBi_2Ta_2O_9$ samples sintered at 1200°C were analyzed, due to higher relative density. Temperature dependence of the real and the imaginary components of the dielectric permittivity, along with dielectric losses (tan d). Curves at 1 MHz (top right) indicate negligible thermal hysteresis during heating/cooling cycles. Frequencies of measurement were: 100 Hz, 500 Hz, 1 KHz, 5 KHz, 10 KHz, 50 KHz, 100 KHz, 500 kHz and 1 MHz (9 frequencies). Arrows in Fig. 9 indicate increasing frequency. The dielectric anomaly associated with the transition from the ferroelectric to the paraelectric phase was observed in all curves (Fig. 9). Curie temperature was $T_c = 315$ ºC, which is in a good agreement with data reported in the literature, typically found between T_c=300 ºC and $T_c = 350$ ºC [7-9, 23, 34, 42-45].

However, at higher temperatures dielectric constants vary markedly with varying frequencies. This is possibly due to the fact that bismuth layered ferroelectric materials contains inherent defects such as oxygen vacancies resulting from the volatilization of Bi_2O_3 during sintering

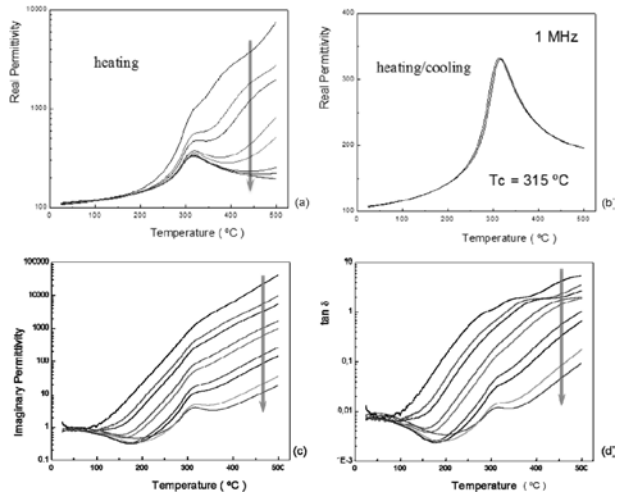

Fig. 9. Temperature dependence of the real and the imaginary components of the dielectric permittivity, along with dielectric losses (tan d), in $SrBi_2Ta_2O_9$ samples sintered by microwave processing at 1200 °C.

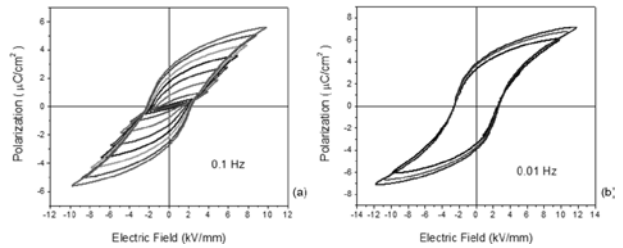

Fig. 10. P-E hysteresis loops in $SrBi_2Ta_2O_9$ samples sintered by microwave processing at 1200 °C.

[32]. To understand the phenomenon of conductivity it is important to note that in addition to the electronic conduction, the oxygen vacancies ($V_{\ddot{o}}$) play a fundamental role, through motion in the crystalline lattice and between the bismuth layer. The molecular formula of $SrBi_2Ta_2O_9$ can be written as $Bi_2O_3.2\{Sr_{1/2}Ta_{1/2}O_{3-\delta}\}$, where represents a vacancy in the A site, as a result of an aliovalent substitution in the lattice, and it is possible to understand the oxygen vacancies ($V_{\ddot{o}}$) as a charge compensation, maintaining the bulk charge neutrality. This is because the oxygen vacancies ($V_{\ddot{o}}$) are charged defects of the opposite sign to a vacancy/charge imbalance in the vacancy. The conductivity of the oxygen vacancies can be expressed as $2e[V_{\ddot{o}}]\mu(T)$, where e is the electronic charge and $\mu(T)$ is the mobility of oxygen vacancies as a function of temperature T. Approaching $2[V_{\ddot{o}}]$ per [A´], according to the charge neutrality, the ionic conductivity $\sigma_{V\ddot{o}}$ due to the constant concentration of oxygen vacancies compensates a net acceptor excess, as shown in Eq. (1),

$$\sigma_{V\ddot{o}} = (\mu^o e[A´] / T) \exp(-H_m / kT) \quad (1)$$

where $\mu^o / T \exp(-H_m / kT)$ represents the ionic mobility and H_m, μ^o, k are the activation energy of the ionic mobility, mobility of the pre-exponential multiplier and Boltzmann`s constant, respectively [10].

The room temperature and maximum permittivity values of 110 and 330, respectively, although slightly lower are also in a good agreement with data reported in the literature [32]. The low-frequency dispersion at high temperatures is also typical of this system, indicating the response is dominated by electrical conduction in this temperature range. Dielectric losses (tan δ) below 0.01 for temperatures lower than 100 °C are suitable for SBT system [32].

Samples sintered by microwave sintering demonstrated a Curie temperature of T_c = 315 ºC that can be directly related to higher density, higher resistivity, better homogenization and finer microstructure. Furthermore, the dielectric constant e_r obtained was around 350 (at T_c), which is consistent with the literature for sintering of SBT ceramics above 900 ºC by conventional processes [46]. In a sample which presents stoichiometric losses, part of the bismuth is removed from the SBT lattice and can migrate to the sample surface, owing to extra oxide bismuth content, which has a vapor pressure of 750 mm Hg at 1570 ºC [34].

It is possible to observe higher dielectric losses at low frequencies. These dielectric losses, in general, can be explained by extended dislocations, grain boundaries or secondary phases. Therefore, avoiding an abnormal grain growth could produce lower dielectric losses using microwave sintering. The dielectric loss of microwave sintered samples is lower compared to conventional sintered samples (Fig. 10(b)) [8-9].

Ferroelectric hysteresis (P-E hysteresis loops) were measured using progressively increasing applied electric fields up to 12 kV/mm at which the electrical breakdown of this sample takes place (Fig. 10). Remnant polarization P_r of 4 mC/cm^2 and coercive field E_c of 2.6 kV/mm were achieved, although the material is far from saturation of the polarization, to which higher electric fields are needed. These values are also typical for ceramics of this system [43]. High voltage sine waves with 0.1 Hz (up to 10 kV/mm) and 0.01 (up to 12 kV/mm) were applied, because of this low frequency waves are better for ferroelectric switching. After hysteresis measurements, a berlincourt d_{33} linear piezoelectric coefficient of 5 pC/N was achieved, which is a typical value for SBT samples sintered by conventional processes [43].

Conclusions

Results show that microwave process proved to be a good alternative to the conventional process to obtain suitable ferroelectric properties. The samples sintered at 1100 ºC were homogeneously microstructural, but revealed lower relative density. On the other hand, the ferroelectric properties of $SrBi_2Ta_2O_9$ samples, with higher relative density, sintered at 1200ºC by microwave processing, revealed a remnant polarization P_r of 4 μC/cm^2, a coercive field E_c of 2.6 kV/mm and a berlincourt d_{33} lineal piezoelectric coefficient of 5 pC/N.

Acknowledgments

The authors acknowledge CAPES for the financial support of this work, CME-UFRGS for the SEM-EDS analysis and the ICMM (Madrid) for the ferroelectric characterization.

References

1. A. Gruverman, A. Kholin, Rep. Prog. in Phys. 69 (2006) 2443-2474.
2. J. Gallego-Juárez, J. Phys. E: Sci. Instrum. 22 (1989) 804-816.
3. J. Zylberberg, A.A. Belik, E. Takayama-Muromachi, Z. Ye. Chem. Mater. 19 (2007) 6385-6390.
4. K. Panda, J. Mater. Sci. 44 (2009) 5049-5062.
5. T.R. Shrout, S.J. Zhang, J. Electroceram. 19 (2007) 113-126.
6. M.D. Maeder, D. Damjanovic, N. Setter, J. Electroceram. 13 (2004) 385-392.
7. T. Chen, C. Thio, S.B. Desu, J. Mater. Res. 12 (1997) 2628-2637.
8. I. Coondoo, A.K. Jha, S.K. Agarwal, J. Electroceram. 16 (2006) 393-398.
9. I. Coondoo, A.K. Jha, S.K. Agarwal, Ceram. International 33 (2007) 41-47.
10. A.R. James, S. Balaji, S.B. Krupanidhi, Mater. Sci. Eng. B 64 (1999) 149-156.
11. B.S. Kang, B.H. Park, S.D. Bu, S.H. Kang, T.W. Noh, Appl. Phys. Lett. 75 (1999) 2644.
12. K. Amanuma, T. Hase, Yoichi Miyasaka, Appl. Phys. Lett. 66 (1995) 221.
13. D. Wang, J. Ceram. Process. Res. 15 (2014) 116-119.
14. Z.Z. Huang, H.L.W. Chan, K.W. Kwok. C.L. Choy, J. Mater. Sci. 35 (2000) 1793-1797.
15. F.F. Oliveira, S. Da Dalt, V.C. Sousa, C. P. Bergmann, Powder Technol. 225 (2012) 239-243.
16. A. Li, D. Wu, H. Ling, M. Wang, X. Yin, Z. Liu, N. Ming, Thin Solid Films 375 (2000) 215-219.
17. J. Lee, B. Park, K. Hong, J. Appl. Phys. 88 (2000) 2825- 2829.
18. C. Fujioka, R. Aoyagi, H. Takeda, S. Okamura, T. Shiosaki, J. Eur. Ceram. Soc. 25 (2005) 2723-2726.
19. H. Amorín, A.L. Kholkin, M.E.V.Costa, J. Eur. Ceram. Soc. 25 (2005) 2453-2456.
20. R. Jain, A.K.S. Chauhan, V. Gupta, K. Sreenivas, J. Appl. Phys. 97 (2005) 124101.
21. P.S. Furtado, M.M. Oliveira, J.S. Vasconcelos, J.H.G. Rangel, E. Longo, V.C. Sousa, Cerâmica 58 (2012) 151-157.
22. G. J. Pereira, D. Gouvêa, Cerâmica 49 310 (2003) 116.
23. V., Senthil, T. Badapanda, A. Chandra Bose, S. Panigrahi, ISRN Ceramics (2012) article ID 943734.
24. Z. Xie, Z. Gui, L. Li, T. Su, Y. Huang, Materials Letters 36 (1998) 191-194.
25. L. Chung-Hsin, C. Yi-Chou, J. Eur. Ceram. Soc. 19 (1999) 2909-2915.
26. T. Atsuki, N. Soyama, T. Yonezawa, K. Ogi, Jpn. J. Appl. Phys. 34 (1995) 5096.
27. M. Noda, Y. Matsumuro, H. Sugiyama, M. Okuyama, Jpn. J. Appl. Phys. 38 (1999) 2275.
28. A.K. Jha, Sugandha, Ferroelectrics 421 (2011) 1-8.
29. P. Thomas, L.N. Sathapathy, K. Dwarakanath, K.B.R. Varma, Bull. Mater. Sci. 30 (2007) 567-570.
30. S. Das, A.K. Mukhopadhyay, S. Datta, D. Basu, Bull. Mater. Sci. 31 (2008) 943-956.
31. M. Oghbaei, O. Mirzaee, J. Alloys Compd. 494 (2010175-189.
32. A.K. Jha Sugandha, Materials Research Bulletin 48 (2013) 1553-1559.
33. A.C. Palanduz, D.M. Smyth, J. Electroceram. 5 (2000) 21-30.
34. Y. Wu, M.J. Forbess, S. Seraji, S.J. Limmer, T. P. Chou, G. Cao, Mater. Sci. Eng. B 86 (2001) 70-78.
35. M.M. Kumar, Z.-G. Ye, J. Appl. Phys. 90 (2001) 934.
36. S. Priya, S. Nahm, Lead-Free Piezoelectrics, Springer, New York, 2012.
37. S.H. Lin, S.L. Swaetz, W.A. Schulze, J.V. Biggers, J. Am. Ceram. Soc. 66 (1983) 881-884.
38. H. Watanabe, T. Kimura, T. Yamaguchi, J. Am. Ceram. Soc. 74 (1991) 139-147.
39. O. Namsar, S. Pojprapai, A. Watcharapasom, S. Jiansirisomboon, J. Appl. Phys. 116 (2014) 164105.
40. P. Nayak, R. Pattanayak, A. Mishra, S. Anwar, P. Sahoo, S. Panigrahi, Metall. Mater. Trans. A 45 (2014) 2132-2141.
41. H. Amorín, V.V. Shvartsman, A.L. Kholkin, M.E.V. Costa, Appl. Phys. Lett. 85 (2004) 5667-5669.
42. J.A. Cho, S. E. Park, T.K. Song, M.H. Kim, H.S. Lee, S.S. Kim, J. Electroceram. 13 (2004) 515-518.
43. Z.Z. Huang, H.L.W. Chan, K.W. Kwok, C.L. Choy, J. Mater. Sci. 35 (2000) 1793-1797.
44. H. Takeda, C. Fujioka, R. Aoyagi, S. Okamura, T. Shiosaki, Appl. Phys. A 81 (2005) 131-135.
45. Y. Shimakawa, Y. Kubo, Y. Nakagawa, S. Goto, T. Kamiyama, H. Asano, F. Izumi, Phys. Rev. B 61 (2000) 6559.
46. 46. J.A. Cho, S.E. Park, T.K. Song, M.H. Kim, H. S. Lee, S.S. Kim, J. Electroceram. 13 (2004) 515-518.